in AML, ALL and CML. Similar events related to treatment with DNA topoisomerase II inhibitors? *Leukemia* 1997; **11**: 1571–4.
9 Tsuzuki M, Handa K, Yamamoto K *et al.* Chronic myeloid leukemia following chemotherapy with 5′-deoxy-5-fluorouridine for gastric cancer. *Intern. Med.* 2008; **47**: 1739–41.
10 Kuhn NZ, Tuan RS. Regulation of stemness and stem cell niche of mesenchymal stem cells: Implications in tumorigenesis and metastasis. *J. Cell. Physiol.* 2010; **222**: 268–77.

ADC Online First, published on November 25, 2013 as 10.1136/archdischild-2013-305037

Clinical and genetic aspects of hypophosphatasia in Japanese patients

Takeshi Taketani,[1,2] Kazumichi Onigata,[2] Hironori Kobayashi,[2] Yuichi Mushimoto,[2] Seiji Fukuda,[2] Seiji Yamaguchi[2]

▶ Additional material is published online only. To view please visit the journal online (http://dx.doi.org/10.1136/archdischild-2013-305037).

[1]Division of Blood Transfusion, Shimane University Hospital, Shimane, Japan
[2]Department of Pediatrics, Shimane University Faculty of Medicine, Shimane, Japan

Correspondence to
Dr Takeshi Taketani, Division of Blood Transfusion, Shimane University Hospital, 89-1, Enya, Izumo, Shimane 693-8501, Japan; ttaketani@med.shimane-u.ac.jp

Received 9 August 2013
Revised 23 September 2013
Accepted 1 November 2013

ABSTRACT

Objective We examined the clinical and genetic features of hypophosphatasia (HPP) in Japanese patients. HPP is a rare metabolic bone disorder of bone mineralisation caused by mutations in the liver/bone/kidney alkaline phosphatase (*ALPL*) gene, which encodes tissue-non-specific alkaline phosphatase isoenzyme.

Methods We retrospectively investigate the incidence and clinical features of 52 patients with paediatric HPP who were born between 1999 and 2010. Mutations of the *ALPL* gene were analysed in 31 patients.

Results The annual incidence of perinatal lethal HPP (PLH) was estimated to be 2–3/1 000 000 births. The most frequent clinical type was PLH followed by prenatal benign. In addition to bone symptoms, cerebral manifestations were frequently observed including convulsion, mental retardation, deafness and short stature with growth hormone deficiency. Respiratory failure was the most significant predictor of a poor prognosis for PLH. The first and second most frequent mutations in the *ALPL* gene were c.1559delT and c.T979C (p.F327L), respectively. The c.1559delT homozygous mutation was lethal with respiratory failure. Patients with the p.F327L compound heterozygous mutation had the different non-lethal type with short stature and a gradual improvement in ALP level and bone mineralisation.

Conclusions The most frequent clinical type was the PLH type with prognosis related to respiratory failure, biochemical/radiological changes and *ALPL* mutations. Cerebral manifestations frequently occurred. Genotype–phenotype correlations were associated with specific outcomes in the PLH type, whereas different clinical features were associated with the same genotype in the non-lethal type.

What is already known

- Hypophosphatasia (HPP) is characterised by defective bone and tooth mineralisation and reduced serum ALP activity.
- The clinical severity of HPP depends on the age of onset.
- The phenotypes of HPP are related to the residual enzyme activity of alkaline phosphatase (ALPL) mutations.

What this study adds

Japanese patients with hypophosphatasia (HPP) have many cerebral manifestations. The most frequent clinical type was the perinatal lethal HPP (PLH) type with prognosis was related to respiratory failure, biochemical/radiological changes and alkaline phosphatase (*ALPL*) mutations. Genotype–phenotype correlations were associated with specific outcomes in the PLH type, whereas different clinical features were associated with the same genotype in the non-lethal type.

INTRODUCTION

Hypophosphatasia (HPP) is a metabolic bone disorder caused by mutations in the liver/bone/kidney alkaline phosphatase (*ALPL*) gene, which encodes tissue-non-specific alkaline phosphatase.[1 2] This disease is characterised by defective bone and tooth mineralisation and reduced serum ALP activity.[1 2] According to several reports from Western populations, HPP patients exhibit autosomal dominant (AD) and autosomal recessive (AR) inheritance, while almost all HPP patients in the Japanese population are AR.[3–6] Patients with AR inheritance have a severe or mild clinical phenotype, whereas those with AD have a mild phenotype.[1–4] The clinical severity of HPP often depends on the age of onset.[2] The five clinical types of HPP are: (1) perinatal which is apparent at birth, (2) infantile from 1 to 6 months, (3) childhood type from the age of 6 months to 18 years, (4) odonto type, which is characterised by the premature loss of deciduous teeth by 5 years without apparent bone symptoms and (5) adult. The perinatal type is usually lethal because of a profound reduction in osteogenesis; half of the patients with the infantile type and all patients with the childhood type survive but experience premature loss of deciduous teeth as well as delayed walking and waddling, which reflect the degree of the skeletal disease.[1 2] However, some patients with prenatal onset, namely the prenatal benign type have ameliorated spontaneous skeletal defects and survive.[2 7 8] Low ALP activity contributes to elevated levels of ALP substrates, that is, pyridoxal 5′-phosphate, phosphoethanolamine (PEA) and inorganic pyrophosphate.[1] More than 260 types of *ALPL* mutations have been identified in HPP patients, and 80% of these are missense mutations according to the *ALPL* mutations database (http://www.sesep.uvsq.fr/03_hypo_mutations.php#mutations). The phenotypes of HPP patients are also closely related to the residual enzyme activity effects of *ALPL* mutations.[9 10] No curative therapy has been established for HPP. Currently, bone-targeted enzyme replacement therapy and cell

To cite: Taketani T, Onigata K, Kobayashi H, *et al. Arch Dis Child* Published Online First: [*please include* Day Month Year] doi:10.1136/archdischild-2013-305037

transplantation from bone marrow and other bone sources are under development.[11–15]

There are very few group-specific or country-specific reports on the clinical and genetic features of HPP in paediatric patients. However, the common *ALPL* mutations observed in Japanese patients, that is, homozygous mutation of c.1559delT and compound heterozygous mutation of c.T979C (p.F327L) have been shown to be associated with relatively lethal and mild types of HPP, respectively.[4–6] Therefore, our study examined the clinical and genetic aspects of HPP in Japanese children.

METHODS

Clinical survey of HPP patients

A questionnaire was sent to approximately more than 500 paediatric medical institutes (95%) throughout Japan to determine the incidence of patients with paediatric HPP born between 1999 and 2010. A thorough review of institutions reporting HPP patients involved the verification of clinical types and features, serum ALP and urine PEA levels in a spot urine collection and radiographic exam information. Clinical features were reviewed from onset to initiation of investigation (June 2010), while biochemical and radiographic tests were performed only at diagnosis. Short stature was defined as −2 SD of height. The diagnostic criteria of growth hormone deficiency (GHD) were as follows: (1) height less than −2.5 SD, (2) insulin-like growth factor-1 less than 200 ng/mL and (3) GH release deficiency in GH secretion test with insulin, arginine or L-3,4-dihydroxyphenylalanine. Assessment of mental retardation was performed by: developmental quotient scores, the Enjoji scale of infant analytical development or IQ. Five clinical types were defined as follows: perinatal lethal HPP (PLH), prenatal benign HPP (PBH), infantile, childhood and odonto. We defined the PLH type as occurrence of a respiratory failure within 1 month after birth and the prenatal benign type as no respiratory failure because other clinical symptoms could not be differentiated between the PLH and PBH types.

ALPL gene analysis

After informed consent was obtained, *ALPL* gene analysis of 31 patients in 52 patients was performed. DNA was extracted from peripheral blood samples and the entire *ALPL* coding region was sequenced by PCR to analyse mutations (Ensembl/Havana merged gene: ENSG00000162551). DNA (50 ng) solution was amplified by PCR in a total volume of 20 µL with 10 mM Tris–HCl (pH 8.3), 50 mM KCl, 1.5 mM $MgCl_2$, 0.001% (wt/vol) gelatin, 5% dimethyl sulfoxide, 250 µM of each deoxynucleotide triphosphates, 2.5 units Taq polymerase (AmpliTaq Gold; Applied Biosystems, Foster City, California, USA) and 10 pmol of each primer. The primers used in these analyses are shown in online supplementary table S1. PCR amplification was performed using a DNA thermal cycler (Applied Biosystems) under the following conditions: initial denaturation at 95°C for 9 min, 35 cycles at 95°C for 30 s, 60°C for 30 s and 72°C for 1 min, followed by a final elongation at 72°C for 7 min. The PCR products were sequenced by the fluorometric method using the BigDye terminator cycle sequencing kit (Applied Biosystems).

RESULTS

Incidence

Paediatric doctor of appropriately 70% hospitals in which we sent the questionnaire replied. The survey collected data from 52 patients. The frequencies of patients with PLH, prenatal PBH, infantile, childhood and odonto type HPP were 21, 14, 5, 9 and 3, respectively. There was neither adult type nor mild HPP with AD fashion. The annual incidence was 2–10 patients each year. The male to female ratio was 33:19 (p=0.055). The number of sporadic and familial patients was 46 and 6, respectively. The incidence of patients with HPP tended to be geographically constrained. In particular, patients were significantly more prevalent in Honshu, the main island of Japan than other islands including Hokkaido, Shikoku, Kyushu and Okinawa (p=0.03).

Clinical type-related characteristics

PLH and PBH types

All patients with PLH and PBH types (n=35) underwent the fetal ultrasonographic examination. Short extremities or deformed limbs and hydramnios were detected in 19/35 of fetuses (54%) (table 1, figure 1). Out of 19 patients with an abnormal fetal echo test, 12 were PLH and 7 PBH. The abnormal ultrasound findings were detected at 20–30 weeks of

Table 1 Clinical and radiographic characteristics of hypophosphatasia

	Perinatal lethal (21)	Prenatal benign (14)	Infantile (5)	Childhood (9)
Clinical findings				
Shortening or deformity of the extremities	15	13	0	4
Bone fracture	3	4	1	0
Respiratory failure	21	0	1	0
Convulsion	9	0	1	2
Enlargement of the anterior fontanelle	4	2	4	0
Renal calcification	3	0	0	0
Short stature	5	8	2	6
Failure to thrive	9	4	5	1
Premature loss of deciduous teeth	5	4	0	3
Mental retardation	5	2	1	3
Premature synostosis of the skull	2	0	2	0
Deafness	5	0	0	0
Radiographic findings				
Hypomineralisation	21	4	5	0
Loss of bone	7	2	0	0
Deformity of long bones	13	12	0	4
Flared metaphyses	13	7	5	1
Hypolucent mid-metaphyses	5	5	1	0
Osteochondral spurs	0	0	0	0
Narrow thorax	19	1	4	0
Biochemical tests				
ALP (IU/L)	20.1	74.8	98	145
Urine PEA (µmol/mg Cr)	7021	2261	1605	873

The alkaline phosphatase (ALP) and urine PEA values are averages. Numbers in parentheses indicate the number of patients. Numbers in brackets indicate biochemical value of ALP and urine PEA. In Japan, the normal blood ALP range is as follows: median 490 IU/L (range=59–921) from birth to 1 month; median 617 IU/L (range=199–1035) during 2–5 months; median 471 IU/L (range=180–762) from 6 months to 1 year. The lower cut-off level during years 1–7 was 170 IU/L. The normal urine PEA range is 31–110 µmol/mg Cr.
PEA, phosphoethanolamine.

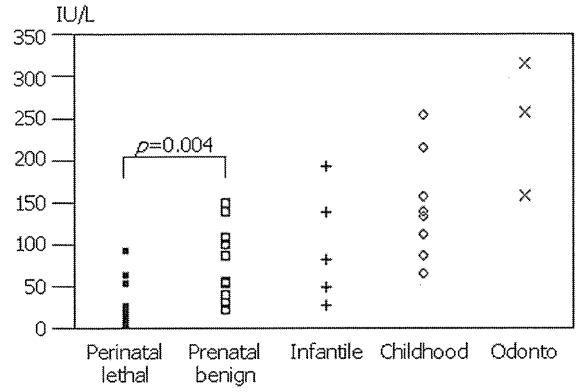

Figure 1 The alkaline phosphatase (ALP) levels of different clinical types.

gestation. The age when diagnosis was confirmed ranged from 0 to 21 days after birth. Two patients were diagnosed 2 weeks after birth because of life-threatening conditions. The main symptoms in both types were short extremities, deformed limbs and bone fractures, short stature, failure to thrive, mental retardation and constipation; respiratory failure, vitamin B6-dependent convulsion, deafness, renal calcification and premature synostosis of the skull occurred only in PLH. Most patients with PLH developed tracheobronchial spasm due to tracheomalacia or bronchomalacia and pulmonary hypertension due to hypercapnia or pulmonary dysfunction. The former condition repeatedly induced severe cyanotic attacks and hypoxic brain damage was recorded. Two of 14 patients with PBH presented with short stature complicated by GHD.

The ALP level was significantly lower in PLH compared with PBH (p=0.0004) (figure 1), while the urine PEA titre was significantly higher in the former (p=0.0035). Radiographic examination showed that significant hypomineralisation and narrow thorax were more frequent in PLH than in PBH (p<0.0001). Osteochondral spurs were not found. In PBH, the ALP titre and urine PEA tended to be gradually increased and decreased, respectively. The hypomineralisation also improved gradually.

According to the prognosis, the median time of death was 4 months (range=0–68 months) in PLH type (figure 2); however, four patients with the PLH type kept survived over 3 years. The main cause of death was respiratory failure. The ALP concentration was significantly lower in PLH type than in PBH (p=0.00187). Respiratory failure (p=0.0001), hypomineralisation (p=0.0008), bone loss (p=0.0021) and narrow thorax

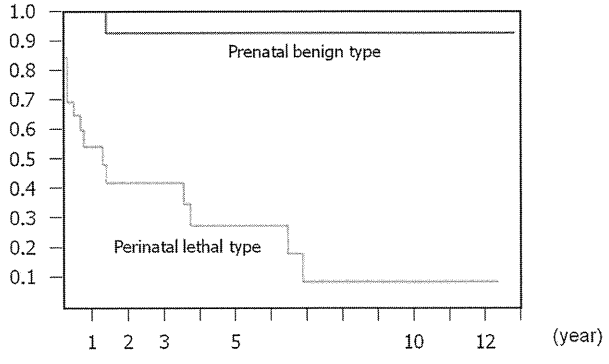

Figure 2 Overall survival rates with respiratory failure (Kaplan–Meier method). The red and green lines indicate patients with and without respiratory failure, respectively.

(p=0.0091) significantly correlated with a poor prognosis, whereas bone shortening/deformity, convulsion and failure to thrive did not. All patients with respiratory failure died within 60 months, with one exception, where respiratory failure developed from a respiratory distress syndrome caused by a premature birth. Another patient of PBH died of viral cardiomyopathy.

Infantile type

No abnormalities were found during the perinatal period in five cases with the infantile form. The age of diagnosis was 2–4 months. All five patients exhibited failure to thrive, hypercalcaemia, hypomineralisation and flared metaphyses which resulted in rickets. For the follow-up period (3–10 years), premature loss of deciduous teeth was not recorded in any cases at the age of 5 years. Only one patient had respiratory failure resulting in death. Two living patients presented with short stature and ambulation difficulty.

Childhood type

The median age was 3 years (range = 10 months to 5 years) at diagnosis. Short extremities, short stature and premature loss of deciduous teeth existed at diagnosis. Mental retardation and convulsion were also recorded. Long bone deformities were found in four patients during radiographic examination. Hypomineralisation and flared metaphyses were not present. All nine patients survived. Three of the six patients with short stature were treated with GH.

Odonto type

The age of diagnosis was 2–4 years. The only clinical symptom was a premature loss of deciduous teeth in all three patients. The median ALP level was 200 IU/L.

Gene analysis

ALPL mutations were identified in 31 patients: 19 perinatal, 5 infantile, 5 childhood and 2 odonto types (table 2). The remaining

Table 2 Genetic analysis of the *ALPL* gene

Clinical types	Genotype	Number of patients
Perinatal lethal type	c.1559delT/c.1559delT	7
	c.1559delT/p.N190del	1
	c.1559delT/p.H324R	1
	c.1559delT/p.G426S	1
	c.1559delT/p.R433C	1
	p.R223Q/p.R272C	1
Prenatal benign type	c.1559delT/p.F327L	2
	p.F327L/p.R428X	1
	p.F327L/p.G439R	1
	p.F327del/p.R184W	1
	p.A40V/p.E191G	2
Infantile type	c.1559delT/p.L299P	2
	c.1559delT/p.F327L	1
	c.1559delT/p.Y436C	1
	p.K224E/p.G426C	1
Childhood type	c.1559delT/ pF327L	3
	p.F327L/p.G339R	1
	p.F327L/p.A111T	1
Odonto type	c.1559delT/p.R136H	2

ALPL, alkaline phosphatase.

21 patients did not receive genetic testing. Two mutant alleles were identified in 31 patients and no heterozygous mutations were found, suggesting that most Japanese HPP cases are the result of AR inheritance. All parents were found to be carriers in the genetic analysis of the parents of 15 patients. Mutations in c.1559delT (29 alleles) and p.F327L (10 alleles) were the frequent mutations. The most frequent Japanese HPP genotype was a homozygous mutation (c.1559delT/c.1559delT), which was observed in seven patients, while the compound heterozygous mutation of c.1559delT/p.F327L was found in six patients. No homozygous mutation of p.F327L was detected. Interestingly, patients with p.F327L were all types except for the PLH type. There is no distortion of the distribution of mutations depending on the island the patients originate.

All seven patients with c.1559delT/c.1559delT had the PLH type with respiratory failure. Five of seven patients with the mutation died, whereas the other two received mechanical ventilation. The frequency of hypominiralisation ($p=0.0299$) and respiratory failure ($p=0.0189$) were significantly higher and the ALP level was significantly lower (28.7 vs 118.4 IU/L, $p=0.0098$) in patients with the homozygous mutation than in patients with other genotypes. Two of the six patients with the compound heterozygous mutation (c.1559delT/p.F327L) had PBH, one had the infantile type and three had the childhood type. All six patients with this genotype survived without serious sequelae but had short stature. Interestingly, siblings of these patients with this genotype had different clinical features. The oldest sibling had the childhood type and a short stature caused by bone deformity, whereas the youngest sibling had PBH, an immunoglobulin A nephropathy and a short stature which was caused by bone deformity and GHD.

DISCUSSION

This retrospective study investigated the clinical and genetic features of HPP in Japanese patients. The epidemiological study found that the perinatal lethal type was the most frequent and was more common in males than in females. The low number of patients with the infantile and childhood types as well as no patients with adult type and mild HPP with AD fashion may have been because HPP remains undiagnosed due to low awareness of HPP. In Japan, the annual incidence of PLH was estimated as about 2–3 patients/1 000 000 births, that is, one case in 300 000–500 000 births with a Japanese birth rate of 1.1 million/year. In Canada, the prevalence in the general population of the most severe forms of HPP is estimated to be ~1:100 000.[16] A molecular-based estimation of the prevalence of HPP in the European population estimated the prevalence of severe HPP and moderate HPP as 1/300 000 and 1/6370, respectively.[3] In the Japanese population, the prevalence of the 1559delT homozygous mutation in the *ALPL* gene, which is a common mutation that causes the perinatal lethal form, was estimated to be not less than 1/900 000.[6] Michigami *et al*[4] reported that c.1559delT represents 40.9% of severe alleles. This mutation was not found in other countries, suggesting that c.1559delT may be a founder mutation in the Japanese population.

Some of the perinatal type cases were diagnosed with HPP during the early gestational period based on ultrasound examination and a positive familial history. However, ultrasound abnormalities early in pregnancy are not necessarily diagnostic for perinatal forms of HPP[8] and may have resulted in elective abortion. Some fetal deaths may also have been the result of HPP. The current retrospective survey was not exhaustive, which is why the number of perinatal type cases may have been underestimated. Thus, a nationwide prospective survey is required to determine the actual incidence of HPP.

Compared with previous reports of HPP clinical characteristics in Western populations,[1 2] the frequency of mental retardation, deafness and short stature were more frequent in Japanese HPP patients, while convulsion was approximately the same. Mental retardation was observed in all types, even when patients did not present complications from hypoxic damage due to respiratory disturbance. The auditory tests were normal at birth, suggesting that deafness was acquired after birth and was not congenital. It is possible that the acquisition of deafness may be exacerbated by hypomineralisation of the ear ossicles. However, auditory brainstem response audiometry showed that the brainstem or cerebral cortex was damaged (data not shown). Short stature was also observed in all HPP types. Interestingly, approximately half of the patients with a short stature had GHD, rather than mineralisation dysfunctions or bone deformities. GHD in all patients was GH release deficiency in GH secretion test with insulin, arginine or L-DOPA, demonstrating that GH-secretion by the pituitary gland was decreased. ALP, present in the neuronal membrane, interacts with the synapses that are involved in neurotransmitter synthesis, synaptic stabilisation and myelin pattern formation; however, there are no reports of GHD in knockout mice.[17–20] Thus, ALP may play a role in developmental plasticity and activity-dependent cortical functions. A study in mice also showed that ALP dysfunction compromises myelination and synaptogenesis in the brain.[20] This suggests that cerebral impairment, including convulsion, mental retardation, deafness and GH deficiency, might be dependent on the severity of the ALP activity as well as the differences in the genetic and ethnic backgrounds of patients.

We designated patients with or without respiratory failure as PLH or PBH, respectively, because prognosis of respiratory failure was worse in the survey. Convulsion, renal calcification, premature synostosis of the skull and deafness were exclusive characteristics of the PLH type and were not poor prognostic predictors. Convulsion may be the best predictor of poor outcome because the follow-up period is short. Patients with the PLH type had significantly lower ALP levels and higher urine PEA levels compared with those with the PBH type. However, ALP and PEA absolute levels did not define the outcome because the cut-off value of ALP and PEA could not be identified. The radiological findings showed that bone mineralisation, flared metaphyses and a narrow thorax were significantly more frequent in the PLH type compared with the PBH type. Interestingly, ALP levels and bone mineralisation gradually increased in the benign type, suggesting that biochemical and radiographic changes need to be assessed over time. All patients with the c.1559delT homozygous mutation had the PLH type, whereas patients with p.F327L had the other types of HPP. Previous reports demonstrated that c.1559delT homozygous and p.F327L heterozygous mutations are associated with lethal and mild types, respectively.[4 5] These suggest that accurate prognosis of Japanese patients with HPP may depend on respiratory condition, biochemical/radiological changes and genetic mutation.

Interestingly, six patients who carried the c.1559delT/p.F327L compound heterozygous mutation were divided into three clinical types: PBH type, infantile type and childhood type. The different onset ages in patients with the same genotype were probably attributable to their initial symptoms. The primary presentation was a long bone deformity based on a fetal echo examination for patients with the PBH type. A bone

fracture was detected initially in patients with the infantile type. Patients with the childhood type were diagnosed based on their short stature or the premature loss of their deciduous teeth. The ALP level increased gradually and bone mineralisation improved gradually in the PBH and infantile types. Short stature was observed in all patients. All patients survived without severe sequelae. Wenkert *et al*[8] also reported that prenatal benign type severity post-natally spanned the 'infantile' to 'odonto' HPP phenotypes and that discordance for prenatal benign type occurred between siblings despite identical *ALPL* mutations. Ozono *et al*[21] proposed a molecular mechanism for the PBH type, suggesting greater expression of the allele harbouring the milder *ALPL* allele defect. The residual enzyme activity effects of *ALPL* mutations, c.1559delT and p.F327L, were none and 70%, respectively.[4] This suggests that patients with c.1559delT/p.F327L compound heterozygous mutations were at different ages at diagnosis, but have experienced the same good clinical course. Further biochemical and physiological investigation would need to clarify why patients with compound heterozygous mutations, c.1559delT/p.F327L, ameliorate.

CONCLUSIONS

This retrospective study investigated the clinical and genetic features of Japanese HPP patients. The incidence of PLH was estimated to be approximately 2–3/1 000 000 births. The most frequent clinical type was PLH, followed by PBH. The Japanese phenotype was frequent central nerve dysfunction including convulsions, mental retardation, deafness and short stature with GHD. We found that lifetime prognosis for HPP was related to respiratory failure, biochemical/radiological changes and *ALPL* mutations. Genotype–phenotype correlations were associated with specific outcomes, although different clinical features with non-lethal type had the same genotype.

Acknowledgements We thank all the Japanese attending physicians for kindly providing the clinical data of patients. We also thank Ms Midori Furui, Mayumi Nagase, Mayumi Naito, Rie Eda and Miho Hattori for analysis of the clinical data and support during molecular analysis.

Contributors TT conceptualised and designed the study, drafted the initial manuscript and approved the final manuscript as submitted. KO managed and designed the study, reviewed and revised the manuscript and approved the final manuscript as submitted. HK carried out the initial analyses, reviewed and revised the manuscript and approved the final manuscript as submitted. YM collected the clinical data and carried out the initial analyses, reviewed and revised the manuscript and approved the final manuscript as submitted. SF performed the genetic analysis of the ALPL gene, reviewed and revised the manuscript and approved the final manuscript as submitted. SY managed and designed the study, reviewed and revised the manuscript and approved the final manuscript as submitted.

Funding This study was supported by the Project for Realisation of Regenerative Medicine, Ministry of Education, Culture, Sports, Science and Technology; and Research on Regenerative Medicine for Clinical Application, Ministry of Health, Labor and Welfare.

Competing interests None.

Patient consent Obtained.

Ethics approval Study approved by the Institutional Review Board.

Provenance and peer review Not commissioned; externally peer reviewed.

REFERENCES

1 Whyte MP. Physiological role of alkaline phosphatase explored in hypophosphatasia. *Ann N Y Acad Sci* 2010;1192:190–200.
2 Mornet E. Hypophosphatasia. *Best Pract Res Clin Rheumatol* 2008;22:113–27.
3 Mornet E, Yvard A, Taillandier A, *et al*. A molecular-based estimation of the prevalence of hypophosphatasia in the European population. *Ann Hum Genet* 2011;75:439–45.
4 Michigami T, Uchihashi T, Suzuki A, *et al*. Common mutations F310L and T1559del in the tissue-nonspecific alkaline phosphatase gene are related to distinct phenotypes in Japanese patients with hypophosphatasia. *Eur J Pediatr* 2005;164:277–82.
5 Ozono K, Michigami T. Hypophosphatasia now draws more attention of both clinicians and researchers: a Commentary on prevalance of c. 1559delT in ALPL, a common mutation resulting in the perinatal (lethal) form of hypophosphatasias in Japanese and effects of the mutation on heterozygous carriers. *J Hum Genet* 2011;56:174–6.
6 Watanabe A, Karasugi T, Sawai H, *et al*. Prevalence of c.1559delT in ALPL, a common mutation resulting in the perinatal (lethal) form of hypophosphatasia in Japanese and effects of the mutation on heterozygous carriers. *J Hum Genet* 2011;56:166–8.
7 Brun-Heath I, Chabrol E, Fox M, *et al*. A case of lethal hypophosphatasia providing new insights into the perinatal benign form of hypophosphatasia and expression of the ALPL gene. *Clin Genet* 2008;73:245–50.
8 Wenkert D, McAlister WH, Coburn SP, *et al*. Hypophosphatasia: nonlethal disease despite skeletal presentation in utero (17 new cases and literature review). *J Bone Miner Res* 2011;26:2389–98.
9 Zurutuza L, Muller F, Gibrat JF, *et al*. Correlations of genotype and phenotype in hypophosphatasia. *Hum Mol Genet* 1999;8:1039–46.
10 Mornet E. Hypophosphatasia: the mutations in the tissue-nonspecific alkaline phosphatase gene. *Hum Mutat* 2000;15:309–15.
11 Nishioka T, Tomatsu S, Gutierrez MA, *et al*. Enhancement of drug delivery to bone: characterization of human tissue-nonspecific alkaline phosphatase tagged with an acidic oligopeptide. *Mol Genet Metab* 2006;88:244–55.
12 Whyte MP, Greenberg CR, Salman NJ, *et al*. Enzyme-replacement therapy in life-threatening hypophosphatasia. *N Engl J Med* 2012;366:904–13.
13 Whyte MP, Kurtzberg J, McAlister WH, *et al*. Marrow cell transplantation for infantile hypophosphatasia. *J Bone Miner Res* 2003;18:624–36.
14 Cahill RA, Wenkert D, Perlman SA, *et al*. Infantile hypophosphatasia: transplantation therapy trial using bone fragments and cultured osteoblasts. *J Clin Endocrinol Metab* 2007;92:2923–30.
15 Tadokoro M, Kanai R, Taketani T, *et al*. New bone formation by allogeneic mesenchymal stem cell transplantation in a patient with perinatal hypophosphatasia. *J Pediatr* 2009;154:924–30.
16 Fraser D. Hypophosphatasia. *Am J Med* 1957;22:730–46.
17 Fonta C, Négyessy L, Renaud L, *et al*. Areal and subcellular localization of the ubiquitous alkaline phosphatase in the primate cerebral cortex: evidence for a role in neurotransmission. *Cereb Cortex* 2004;14:595–609.
18 Fonta C, Negyessy L, Renaud L, *et al*. Postnatal development of alkaline phosphatase activity correlates with the maturation of neurotransmission in the cerebral cortex. *J Comp Neurol* 2005;486:179–96.
19 Négyessy L, Xiao J, Kántor O, *et al*. Layer-specific activity of tissue non-specific alkaline phosphatase in the human neocortex. *Neuroscience* 2011;172:406–18.
20 Hanics J, Barna J, Xiao J, *et al*. Ablation of TNAP function compromises myelination and synaptogenesis in the mouse brain. *Cell Tissue Res* 2012;349:459–71.
21 Ozono K, Yamagata M, Michigami T, *et al*. Identification of a novel missense mutations (Phe310Leu and Gly439Arg) in a neonatal case of hypophosphatasia. *J Clin Endocrinol Metab* 1996;81:4458–61.

Clinical and genetic aspects of hypophosphatasia in Japanese patients

Takeshi Taketani, Kazumichi Onigata, Hironori Kobayashi, et al.

Arch Dis Child published online November 25, 2013
doi: 10.1136/archdischild-2013-305037

Notes

Biochemical and Biophysical Research Communications 438 (2013) 753–759

Contents lists available at ScienceDirect

Biochemical and Biophysical Research Communications

journal homepage: www.elsevier.com/locate/ybbrc

N-Cadherin is a prospective cell surface marker of human mesenchymal stem cells that have high ability for cardiomyocyte differentiation

Hisako Ishimine [a,b], Norio Yamakawa [a], Mari Sasao [c], Mika Tadokoro [c], Daisuke Kami [d], Shinji Komazaki [e], Makoto Tokuhara [f], Hitomi Takada [a], Yoshimasa Ito [a], Shinichiro Kuno [g], Kotaro Yoshimura [g], Akihiro Umezawa [d], Hajime Ohgushi [c], Makoto Asashima [a,h,i,*], Akira Kurisaki [a,b,*]

[a] Research Center for Stem Cell Engineering, National Institute of Advanced Industrial Science and Technology (AIST), Tsukuba, Ibaraki, Japan
[b] Graduate School of Life and Environmental Sciences, The University of Tsukuba, Tsukuba, Ibaraki, Japan
[c] Health Research Institute, National Institute of Advanced Industrial Science and Technology (AIST), Amagasaki, Hyogo, Japan
[d] Department of Reproductive Biology and Pathology, National Research Institute for Child Health and Development, Setagaya, Tokyo, Japan
[e] Department of Anatomy, Saitama Medical School, Iruma, Saitama, Japan
[f] Department of Surgery, Research Institute National Center for Global Health and Medicine, Shinjuku, Tokyo, Japan
[g] Department of Plastic Surgery, University of Tokyo School of Medicine, Bunkyo, Tokyo, Japan
[h] Department of Life Sciences (Biology), Graduate School of Arts and Sciences, The University of Tokyo, Meguro, Tokyo, Japan
[i] Life Science Center of TARA, The University of Tsukuba, Tsukuba, Ibaraki, Japan

ARTICLE INFO

Article history:
Received 13 July 2013
Available online 27 July 2013

Keywords:
N-cadherin
Flk-1
c-Kit
Cardiomyocyte
Mesenchymal stem cells

ABSTRACT

Mesenchymal stem cells (MSCs) are among the most promising sources of stem cells for regenerative medicine. However, the range of their differentiation ability is very limited. In this study, we explored prospective cell surface markers of human MSCs that readily differentiate into cardiomyocytes. When the cardiomyogenic differentiation potential and the expression of cell surface markers involved in heart development were analyzed using various immortalized human MSC lines, the MSCs with high expression of N-cadherin showed a higher probability of differentiation into beating cardiomyocytes. The differentiated cardiomyocytes expressed terminally differentiated cardiomyocyte-specific markers such as α-actinin, cardiac troponin T, and connexin-43. A similar correlation was observed with primary human MSCs derived from bone marrow and adipose tissue. Moreover, N-cadherin-positive MSCs isolated with N-cadherin antibody-conjugated magnetic beads showed an apparently higher ability to differentiate into cardiomyocytes than the N-cadherin-negative population. Quantitative polymerase chain reaction analyses demonstrated that the N-cadherin-positive population expressed significantly elevated levels of cardiomyogenic progenitor-specific transcription factors, including *Nkx2.5*, *Hand1*, and *GATA4* mRNAs. Our results suggest that N-cadherin is a novel prospective cell surface marker of human MSCs that show a better ability for cardiomyocyte differentiation.

1. Introduction

Stem cell therapy is expected to be an alternative regenerative medicine. In addition to embryonic stem (ES) cells and induced pluripotent stem (iPS) cells, mesenchymal stem cells (MSCs) have been shown to differentiate into various cell types including osteoblasts, chondrocytes, adipocytes, neurons, skeletal muscle fibers, and cardiomyocytes *in vitro*. However, the differentiation ability of MSCs toward cardiomyocytes is still limited [1–3]. To overcome this problem, cell surface markers specific for cardiomyogenic progenitor cells could be used to enrich better population for regenerative medicine of heart failure.

Flk-1, a vascular endothelial growth factor receptor (VEGFR2), has been reported to be a prospective cell surface marker of cardiomyocyte progenitor cells during heart development [4,5]. Flk-1 is expressed in the progenitors of multiple mesodermal lineages, including cardiac, endothelial, and vascular smooth muscle cells [5]. c-Kit (CD117) is a transmembrane tyrosine kinase receptor for Stem cell factor, and used as a cell surface marker for hematopoietic progenitors, melanocytes, mast cells, and spermatogonial stem cells. Recent research has suggested that c-Kit could be a putative cell surface marker for cardiomyogenic progenitor cells in the neonatal heart [6].

A Ca^{2+}-dependent cell–cell adhesion molecule, N-cadherin, is also expressed on cardiomyocyte progenitor cells during mouse development. N-Cadherin expression is observed in the precardiac

* Corresponding authors. Address: Research Center for Stem Cell Engineering, National Institute of Advanced Industrial Science and Technology (AIST), Tsukuba AIST Central 4-1-3105, Higashi 1-1-1, Tsukuba, Ibaraki, 305-8562, Japan. Fax: +81 29 861 2987.
E-mail addresses: asashi@bio.c.u-tokyo.ac.jp (M. Asashima), akikuri@hotmail.com (A. Kurisaki).

0006-291X/$ - see front matter © 2013 Elsevier Inc. All rights reserved.
http://dx.doi.org/10.1016/j.bbrc.2013.07.081

mesoderm at E8.5 in mice and continues to be expressed in the whole heart during development. N-Cadherin-knockout mice died by E10 because of defects in the primitive heart. Although myocardial tissue was initially formed in the knockout mouse embryos, the myocytes were subsequently dissociated, and the heart tube failed to develop [7].

In this study, we explored cell surface markers of human MSCs that have a high ability to differentiate into cardiomyocytes. We show that N-cadherin is a prospective cell surface marker of MSCs with high cardiomyogenic potential.

2. Materials and methods

2.1. Cell culture

Human MSC cell lines, UE7T-13, UE6E7T-11, UBE6T-15, UE6E7T-12, UE7T-9, and UE6E7T-2, were obtained from the JCRB Cell Bank (Osaka, Japan). They were immortalized by retrovirus gene transfer of a combination of *bmi-1*, *E6*, *E7*, and/or *hTERT* genes to human bone marrow stromal cells harvested from a 91-year-old woman [8,10]. The EPC-214 cell line was similarly immortalized at the National Research Institute for Child Health and Development (NRICHD), Japan [9]. These cell lines were maintained in DMEM high glucose (Wako) supplemented with 10% fetal calf serum (FCS; Roche). As for the primary MSCs, ANP0425 and 0607NC, were obtained from Dr. Ohgushi (National Institute of Advanced Industrial Science and Technology, Japan). MSC-R36_2 cells, MSC-R36_3 cells, and Yub623 cells were obtained from the RIKEN BRC Cell Bank (Ibaraki, Japan). Primary MSCs derived from adipose tissue (ASCs), including 09-036 (36) cells, 10-008 (8) cells, 05-055 (55) cells, and 05-076 (76) cells, were prepared at the University of Tokyo, School of Medicine Tokyo, Japan. KN-SC (KN) cells, MY-SC (MY) cells, and NN-SC (NN) cells were prepared at the Research Institute National Center for Global Health and Medicine (NCGM), Japan. Other ASCs were purchased from Invitrogen. For the ASCs, all samples except KN-SC were obtained from women aged 22–45 years (KN-SC was derived from a 41-year-old man). All of these primary cells were maintained in MesenPRO RS Basal Medium supplemented with MesenPRO RS Growth Supplement (GIBCO). Cells were maintained in a humidified incubator at 37 °C with an atmosphere of 5% CO_2. All the experiments using human materials were approved by the Human Ethics Committee at AIST, NRICHD, NCGM, and the University of Tokyo. Human umbilical vein endothelial cells (HUVEC) were cultured in RPMI-1640 supplemented with EGM-2 SingleQuots (LONZA) and penicillin/streptomycin (Wako). TF-1 cells were cultured in RPMI-1640 supplemented with 10% FBS, 2 ng/mL rhGM-CSF, and penicillin/streptomycin (Wako).

2.2. Preparation of mouse fetal cardiomyocytes

The fetal hearts of E16.5 ICR mice were cut into small pieces and washed with phosphate-buffered saline (PBS). They were incubated with 0.15% trypsin and 0.012% EDTA in PBS at 37 °C for 10 min under gentle stirring. The supernatant containing the dissociated cardiomyocytes was mixed with DMEM supplemented with 10% FCS, and centrifuged at 1000 rpm for 5 min. The pellet was then re-suspended in 10 mL of DMEM with 10% FCS and incubated on a glass dish for 1 h to remove fibroblasts. The floating cardiomyocytes were collected and re-plated at $5 \times 10^5/cm^2$ on gelatin-coated glass bottom dishes (Asahi Techno Glass). All the experiments using animals were approved by the Animal Experiment Committee at AIST.

2.3. Immunoblotting analysis

Human MSC cell lines were homogenized in a lysis buffer containing 20 mM Tris–HCl (pH 7.4), 300 mM NaCl, 0.5 mM EDTA, 1% NP-40, and a complete protease inhibitor cocktail (Roche). After centrifugation at 13,000 rpm for 10 min at 4 °C, equal protein amounts were separated by SDS–PAGE (5–20%). The blots were incubated with antibodies against N-cadherin (1:200; C3865, Sigma), Flk-1 (1:100, 10347; IBL), c-Kit (1:200, AF332; R&D Systems), Integrin-α4 (1:200; sc-14008, Santa Cruz), VCAM-1 (1:200; sc-8304, Santa Cruz), PDGFRα (1:200; 323503, BioLegend), Nkx2.5 (1:200; sc-14033, Santa Cruz), GATA4 (1:200; sc-9053, Santa Cruz), or β-tubulin (1:1000, RB-9249; NeoMarkers). Proteins were detected with an enhanced chemiluminescence (ECL) reagent (Super-Signal West Femto Maximum Sensitivity Substrate, Pierce) using an LAS-3000 Image Analyzer (Fuji Film).

2.4. Flow cytometry analysis

All MSCs were harvested with cell dissociation buffer (GIBCO) and blocked with normal sheep IgG on ice for 1 h. Cells were incubated with biotinylated anti-N-cadherin antibody (1:100, BAF1388; R&D System), anti-Flk-1 antibody (1:100, 10347; IBL), and APC-conjugated anti-c-Kit antibody (1:100, 550412; Becton Dickinson) on ice for 1 h. The N-cadherin antibody was fluorescently labeled using Allophycocyanin-Alexa Fluor 750 streptavidin (Molecular Probes). The Flk-1 antibody was fluorescently labeled with the Alexa Fluor 488-conjugated secondary antibody (Molecular Probes). Cells were resuspended in buffer with propidium iodide (Sigma). Analysis was performed with a FACS Aria (Becton Dickinson) and FlowJo software (TOMY Digital Biology) with propidium iodide-negative population. The data were obtained from at least two independent experiments.

3. Results

MSCs are a mixture of primary adherent cells derived from the stroma of adult tissues. The multipotency of MSCs rapidly decreases as the passage number increases. Therefore, it is not easy to obtain reproducible data from these heterogeneous primary cells. To overcome these problems, we took advantage of immortalized human MSC clones with *bmi-1*, *TERT*, *E6*, and/or *E7*, which retain their multipotent differentiation ability over a long time when cultured *in vitro* [8].

Cardiac differentiation of human MSCs was performed by co-culturing with mouse fetal cardiomyocytes, which is a well-established method to differentiate MSCs into electro-physiologically validated cardiomyocytes [9,10]. Human MSC cell lines were labeled with a GFP-expressing lentivirus and then cultured on a cardiomyocyte feeder cells prepared from mouse embryonic heart tissue (Fig. S1A). On day 7, human MSC lines such as EPC-214 and UE7T-13 differentiated into cardiomyocytes. Around 5% of these GFP-labeled MSCs differentiated into beating cardiomyocytes (Fig. 1A). GFP-positive, differentiated cardiomyocytes showed autonomously periodical contractions (Fig. S1B). Significant number of GFP-positive human MSCs expressed cardiomyocyte-specific terminal differentiation markers (Fig. S1C, left and middle, Fig. S1D, left, and a confocal image Fig. S1E). On the other hand, some cell lines did not differentiate into beating cardiomyocytes under identical conditions (UE7T-9, UE6E7T-2) (Fig. S1C right and Fig. S1D right).

Next, the efficiency of human MSCs differentiation into spontaneously beating cardiomyocytes was quantified by counting the number of GFP-positive and spontaneously beating cardiomyocytes with a fluorescence microscope on day 7 (Fig. 1A). The

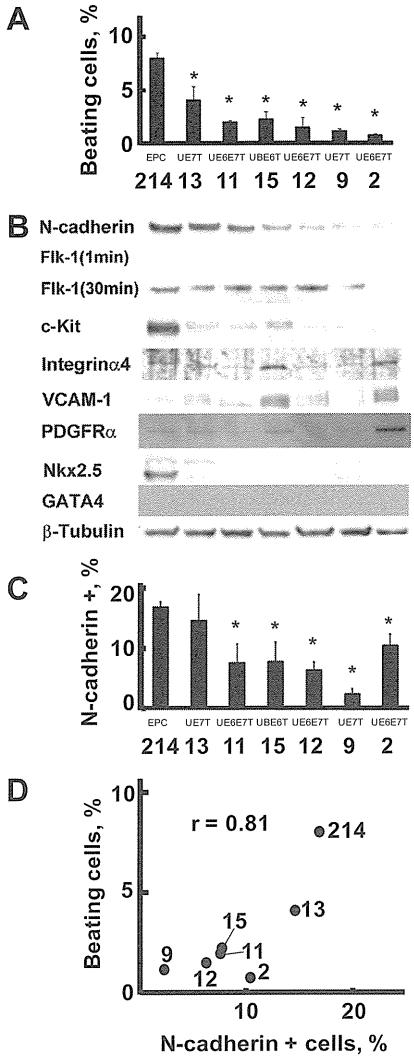

Fig. 1. Correlation between cardiomyogenic differentiation efficiency and cell surface protein marker expression in human MSC cell lines. (A) Autonomously beating cardiomyocytes differentiated from GFP-labeled human MSC lines, EPC-214, UE7T-13, UE6E7T-11, UBE6T-15, UE6E7T-12, UE7T-9, and UE6E7T-2, were counted under a fluorescence microscope. (B) The expression of cell surface proteins and transcription factors related to cardiovascular development were analyzed by immunoblotting of whole cell lysates. (C) Flow cytometric analysis of cell surface expression of N-cadherin in human MSC lines. (D) Correlation between the differentiation efficiency into cardiomyocytes and cell surface N-cadherin expression in human MSC lines. The vertical axis represents the differentiation efficiency. The horizontal axis represents cell surface expression of N-cadherin. The correlation coefficient (r) is shown on the graph. $^{*}P < 0.05$.

expression of various cell surface proteins, which are essential for the development of the heart *in vivo* or are specifically expressed in cardiovascular progenitor cells, was examined by immunoblotting (Fig. 1B). Among these markers, the expression of N-cadherin showed a good correlation with the differentiation efficiency toward beating cardiomyocytes. The MSC lines highly expressing N-cadherin showed higher differentiation ability toward cardiomyocytes. Flk-1 also showed an expression pattern similar to that of N-cadherin. However, the expression levels in human MSCs were very low. Only an extremely long exposure (30 min) enabled us to detect the Flk-1 protein bands (Fig. 1B). The expression of c-Kit showed some correlation with the cardiomyogenic differentiation abilities of these cells, although the expression levels of c-Kit in some human MSCs that readily differentiated into cardiomyocytes were very low (Fig. 1B, UE7T-13, UE6E7T-11, and UBE6T-15).

Other cell surface proteins have been reported as essential for heart development. Integrin α4 is essential for the development of the heart and placenta [11]; a homozygous null mutant of integrin α4 caused embryonic lethality due to defects in the epicardium and coronary vessel development, leading to cardiac hemorrhage, in addition to failure of fusion between the allantois and chorion during placentation. Knockout mice of vascular cell adhesion molecule 1 (VCAM-1) displayed a reduction in the compact layer of the ventricular myocardium and intraventricular septum [12]. Platelet-derived growth factor receptor α (Pdgfrα) is expressed in cardiac progenitor cells in the posterior part of the secondary heart field. Pdgfrα is also expressed in the valves and pericardia of the heart at E12.5–16.5 [13]. However, the expression of these cell surface proteins did not show a strong correlation with the differentiation ability of human MSCs into cardiomyocytes (Fig. 1A and B).

Next, we verified the cell surface-specific expression of N-cadherin, Flk-1, and c-Kit in living MSCs by flow cytometry. Flk-1 was barely detectable on the cell surface of human MSCs (Fig. 2A), although a positive control, HUVEC, showed strong cell surface expression of Flk-1 (Fig. 2A, right), indicating that human MSCs do not express detectable amounts of Flk-1 on the plasma membrane. The cell surface expression of c-Kit was also relatively low (Fig. 2B), and the MSC lines with higher differentiation ability toward cardiomyocytes did not show a significant amount of cell surface expression of c-Kit (Fig. 2B, UE7T-13).

By contrast, N-cadherin was readily detectable in the human MSC lines with high differentiation ability toward beating cardiomyocytes (Fig. 2C). When the cell surface expression of N-cadherin (Fig. 1C) and the differentiation ability into beating cardiomyocytes (Fig. 1A) were compared with human MSC cell lines, a strong correlation was observed between these 2 events ($r = 0.81$; Fig. 1D). Immunofluorescence analysis of the human MSC line EPC-214, which readily differentiated into cardiomyocytes, showed characteristic localization of N-cadherin in cell-to-cell contacts in addition to the uniform expression on the plasma membrane (Fig. 2D). However, UE7T-9 cells, which expressed N-cadherin at low levels and did not differentiate into cardiomyocytes, did not show significant expression of N-cadherin (Fig. 2D, right). These results suggest that N-cadherin could be a good prospective cell surface marker of cardiomyogenic human MSCs.

Next, we validated the expression of N-cadherin with various primary human MSCs. Human bone marrow-derives MSCs (BMSCs) cultured for a limited number of passages gave a good correlation between the cell surface expression of N-cadherin and the differentiation ability into beating cardiomyocytes (Fig. 3A and B). Human MSCs derived from adipose tissue (ASCs) also showed similar results (Fig. 3D and E). The Pearson's correlation coefficients of cell surface expression of N-cadherin and differentiation efficiency toward beating cardiomyocytes in BMSCs and ASCs were good in both cases (0.55 and 0.77, respectively; Fig. 3C and F). As for c-Kit, we failed to detect significant expression of c-Kit in primary MSCs that showed distinct cardiomyogenic differentiation abilities (Fig. S2, 36_2). c-Kit protein could be detected on the cell surface of some primary ASCs (Fig. S2B, 1212). However, the isolation of c-Kit-positive cells from these primary ASCs was not successful by flow cytometry.

To determine whether the N-cadherin-positive population of human MSCs has higher differentiation ability into cardiomyocytes than N-cadherin-negative MSCs, we established the separation conditions of N-cadherin-positive cells using MACS (Fig. S3). Then, the N-cadherin-positive fraction was concentrated from a primary culture of human ASCs (1212 used in Fig. 3) using the same method (Fig. 4A); these cells were further cultured on mouse embryonic heart feeder cells for 7 days. The enriched ASC fraction expressing cell surface N-cadherin showed a 4-fold higher cardiomyogenic differentiation ability than the N-cadherin-negative fraction (Fig. 4B).

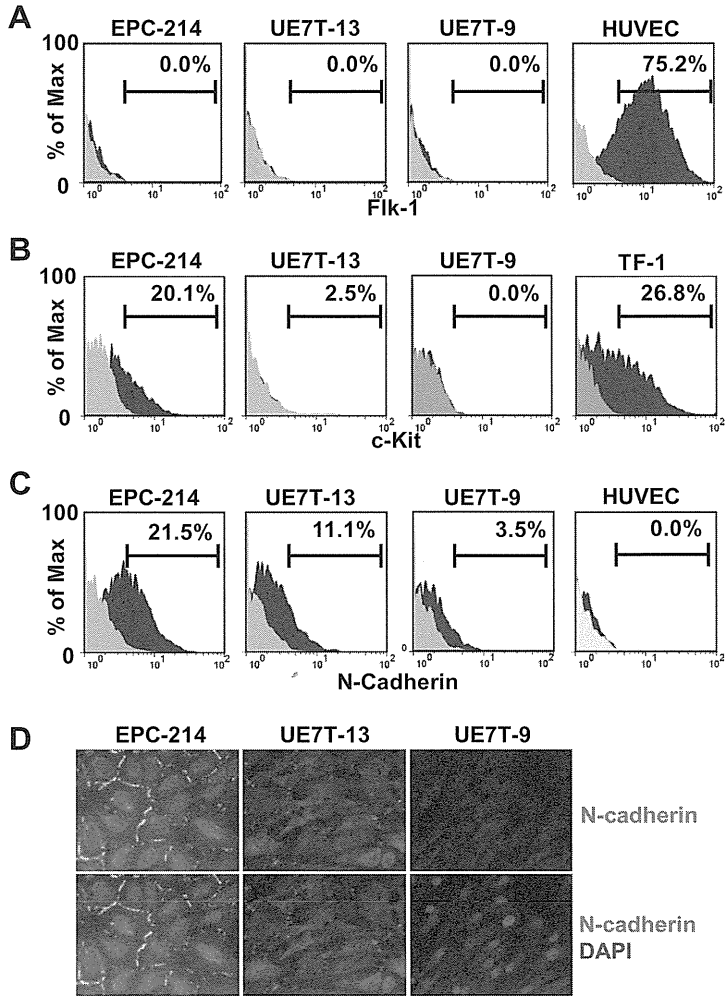

Fig. 2. Representative FACS plots of cell surface protein expression in human MSC cell lines. The live cells were immunostained with (A) Flk-1, (B) c-Kit, or (C) N-cadherin antibodies. Propidium iodide-positive cells were excluded from the analysis. (D) Localization of N-cadherin in human MSCs. The indicated human MSC lines were immunostained with N-cadherin antibody (green) and DAPI (blue). (For interpretation of the references to colour in this figure legend, the reader is referred to the web version of this article.)

To characterize the cardiomyogenic N-cadherin-positive population, we analyzed the gene expression profiles of the MACS-sorted fractions with microarray. Gene ontology analysis of 3056 genes (among 44,000 genes) that exhibited more than a 1.5-fold difference identified molecular functions associated with zinc ion binding, transition metal ion binding, and nucleic acid binding (Fig. S4A) and biological functions involved in DNA binding, gene expression, transcription, and metabolic processes of nucleic acid (Fig. S4B). These results suggested that N-cadherin-positive cells showed higher expression of specific DNA-binding proteins and elevated metabolic activity. On the other hand, the N-cadherin-negative population showed higher expression of genes involved in the MHC class I protein complex, vacuole organization, and GTPase activity (Fig. S4C and S4D).

When the expression of various lineage marker genes was compared, the N-cadherin-positive fraction showed up-regulated expression of genes involved in the differentiation of cardiomyocytes and skeletal myocytes, such as *Nkx2.5*, *Hand1*, *Tnni3* (*cTnI*), and *Myog* (Fig. 4C). In contrast, ectodermal and endodermal lineage markers were the same among the MACS-sorted fractions, with the exception of *Pax4*, a transcription factor involved in pancreatic development. Although MSCs efficiently differentiate into osteoblasts, chondrocytes, and adipocytes, these specific markers did not show a large difference. The expression of MSC-specific cell surface markers was not increased in the N-cadherin-positive fraction.

Quantitative PCR analysis revealed significant up-regulation of a cardiomyogenic precursor-specific gene, *Nkx2.5*, in the N-cadherin-positive fraction, for more than 200-times higher than that in the N-cadherin-negative fraction. Two other transcription factors, *Hand1* and *Gata4*, but not Tbx5, also showed significantly elevated expression in the N-cadherin-positive fraction (Fig. 4D). Interestingly, the expression of *Myog*, a transcription factor involved in skeletal muscle development, was also elevated in the N-cadherin-positive fraction. Although terminal markers for cardiomyocytes, such as *Anp* and *cTnI*, showed higher expression in the N-cadherin-positive fraction (Fig. 4E), the expression levels of these terminal markers were very low, suggesting that N-cadherin-positive cells may be ready for differentiation, but not terminally differentiated into cardiomyocytes.

Interestingly, the expression of some pluripotency-specific genes such as *Oct4* (*Pou5f1*), *Sall4*, and *Nanog* was significantly up-regulated in the N-cadherin-positive population (Fig. 4F and G). However, these expression in human MSCs was not as high as that in human ES cells (Fig. 4F), suggesting that these genes up-regulated in N-cadherin-positive MSCs may not exhibit pluripotency as observed in ES/iPS cells.

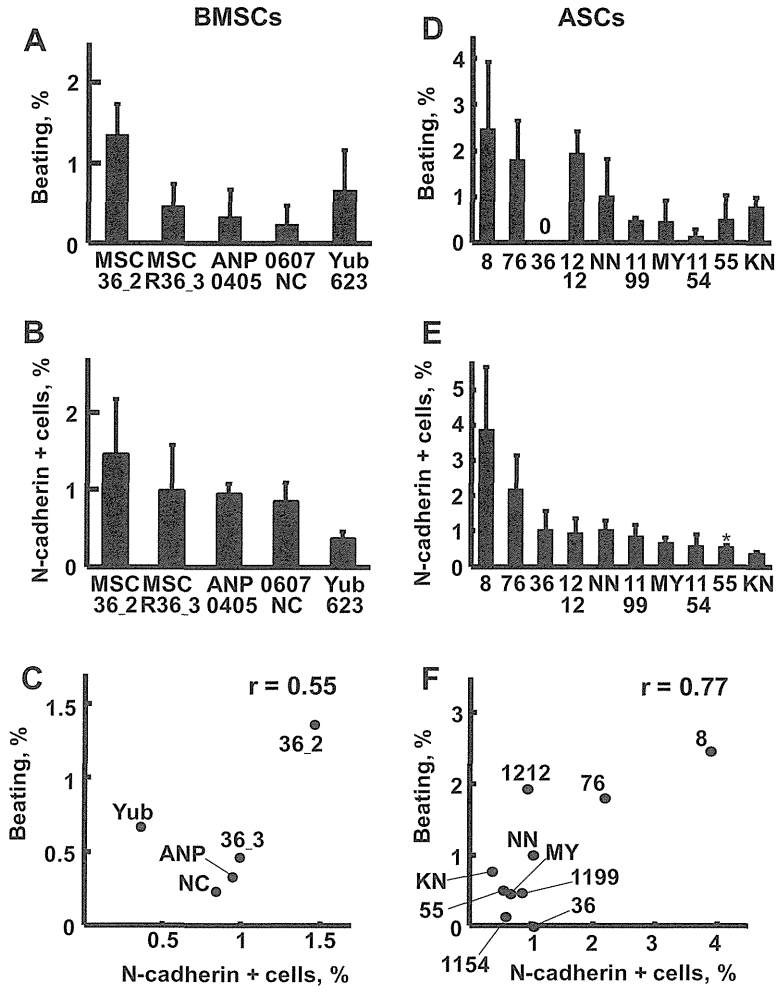

Fig. 3. Differentiation efficiency of primary human MSCs into cardiomyocytes and cell surface expression of N-cadherin. In this experiment, primary human MSCs derived from (A–C) the bone marrow (BMSCs) or (D–F) adipose-derived tissue (ASCs) were used. (A, D) Differentiation efficiency of primary human MSCs into cardiomyocytes. Autonomously beating cardiomyocytes differentiated from GFP-labeled human (A) BMSCs or (D) ASCs were counted using a microscope. (B, E) Flow cytometric analysis of cell surface expression of N-cadherin in primary human (B) BMSCs or (E) ASCs. $^{*}P < 0.05$. (C, F) Correlation between the differentiation efficiency into beating cardiomyocytes and the cell surface N-cadherin expression of primary human (C) BMSCs or (F) ASCs. The correlation coefficient (r) is shown on the graph.

4. Discussion

In this study, we have identified N-cadherin as a reliable cell surface marker for human MSCs with higher differentiation ability toward cardiomyocytes. N-cadherin is continuously expressed from cardiomyogenic progenitor cells to mature cardiomyocytes in the adult heart. N-cadherin maintains the functional gap junction complex at the plasma membrane in the adult heart, and conditional knockout of N-cadherin in mice resulted in arrhythmia in adult hearts with significant decreases in Cn43 and Cn40 [17].

We have previously shown that the cardiomyogenic progenitor cells differentiated from mouse ES cells expressed high levels of N-cadherin on the cell surface membrane, and an antibody against N-cadherin could be used to concentrate the progenitor cells from a heterogeneous cell population differentiated from mouse ES cells [18]. Although the possible differentiation pathway of cardiomyocytes from pluripotent ES cells and multipotent MSCs may not be the same, N-cadherin could be a common progenitor marker of the cardiomyogenic cells derived from these stem cells.

In addition to cardiomyogenic genes, we observed increased expression of pluripotency-specific transcription factors of ES cells, such as *Oct4*, *Sall4*, and *Nanog*, in the N-cadherin-positive fraction. Recently, *Oct4* has been suggested to be the gatekeeper into and out of the reprogramming expressway [19]. Therefore, the elevated expression of *Oct4* and related transcription factors could positively modulate the differentiation ability of MSCs. For example, overexpression of the *Oct4* gene enhanced the differentiation ability of MSCs [14], and knockdown of *Oct4* caused loss of multiple differentiation potential [15]. Nanog was also shown to possess similar activity in BMSCs [16]. Therefore, N-cadherin-positive cells with up-regulated expression of *Oct4* and other transcription factors responsible for cardiomyogenesis may increase the differentiation ability of MSCs into cardiomyocytes.

N-Cadherin is localized in the cell–cell contacts of cardiomyocytes and plays essential roles for formation of the cardiac intercalated disk structure that electromechanically couples adjacent cardiac myocytes. Addition of antibodies against N-cadherin to the cultured cardiomyocytes [20], mesodermal explants [21] or injected into embryos [22] caused a reduction in the number of myofibrils and destroy stress fibers [23]. In primary cardiomyocytes dissociated from adult rat heart, N-cadherin diffusely distributed around the cell periphery begins to co-localize with desmocollin, plakoglobin, and plakophilin-2 at the cell contact sites. The newly generated adhesive contacts sequentially recruit desmoplakin, intermediate filaments, connexin-43, and ankyrin-G. Subsequently, the voltage-gated sodium channel is incorporated into mature intercalated disks. This assembly process requires the clustering of transmembrane adhesive contacts with N-cadherin

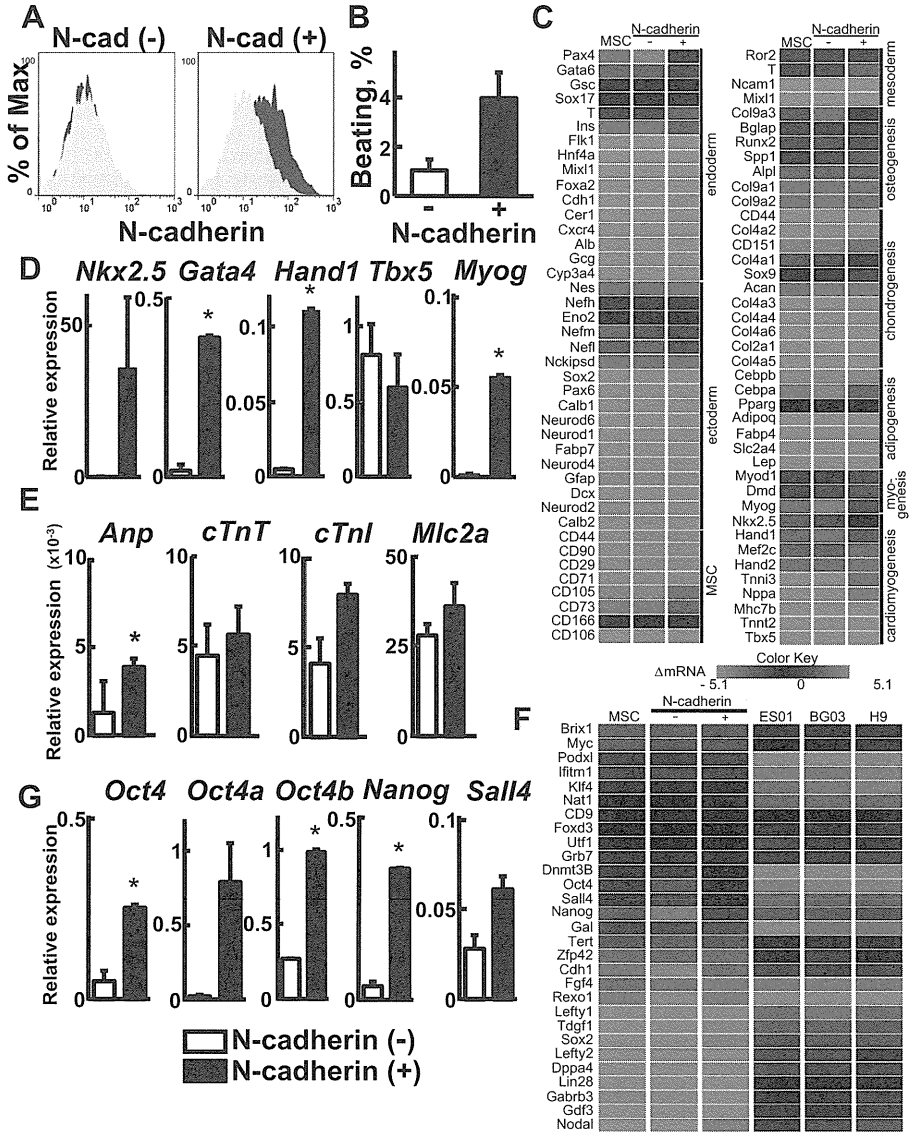

Fig. 4. Separation of N-cadherin-positive cells from the primary MSCs derived from adipose tissue (1212) with anti-N-cadherin antibody-conjugated magnetic beads. (A) The FACS histograms represent cell surface N-cadherin expression in the N-cadherin-negative fraction (left) and N-cadherin-positive fraction (right). (B) Differentiation efficiency of the purified primary ASCs into beating cardiomyocytes. Bar graphs represent the mean value of differentiation efficiency obtained from two independent experiments. (C) Heat map profile of lineage-specific differentiation marker expression in ASCs. The N-cadherin-positive fraction showed elevated expression of specific genes involved in cardiomyogenesis. (D, E) qPCR analysis of cardiomyogenic progenitor-specific transcription factors (D) and terminal differentiation markers for heart development (E). (F) Heat map profile of pluripotency-specific marker expression in human ASCs and human ES cells (ES01, BG03, and H9). (G) qPCR analysis of the expression of pluripotency-specific transcription factors in MACS-sorted fractions. $^{*}P < 0.05$. (For interpretation of the references to colour in (C) and (F), the reader is referred to the web version of this article.)

[24]. Therefore, MSCs with higher expression of N-cadherin may have preferable potential for the differentiation into cardiomyocytes. N-cadherin is expressed in pericytes and is involved in the interaction between pericytes and endothelial cells during vessel formation *in vivo* [25,26]. Pericytes in MSCs could be one of the possible cell sources that show higher differentiation ability toward cardiomyocytes.

Disclosure statement

No competing financial interests exist.

Acknowledgments

We would like to thank to Dr. Yuzuru Ito for discussion. The lentiviral vector for GFP was provided by Dr. Miyoshi (Riken BRC) through the National Bio-Resource Project of the MEXT, Japan. This research was supported by NEDO of Japan (New Energy and Industrial Development Organization, Translational Research Promotion Project).

Appendix A. Supplementary data

Supplementary data associated with this article can be found, in the online version, at http://dx.doi.org/10.1016/j.bbrc.2013.07.081.

References

[1] M. Shiota, T. Heike, M. Haruyama, S. Baba, A. Tsuchiya, H. Fujino, H. Kobayashi, T. Kato, K. Umeda, M. Yoshimoto, T. Nakahata, Isolation and characterization of bone marrow-derived mesenchymal progenitor cells with myogenic and neuronal properties, Exp. Cell Res. 313 (2007) 1008–1023.

[2] S. Wakitani, T. Saito, A.I. Caplan, Myogenic cells derived from rat bone marrow mesenchymal stem cells exposed to 5-azacytidine, Muscle Nerve 18 (1995) 1417–1426.

[3] S. Makino, K. Fukuda, S. Miyoshi, F. Konishi, H. Kodama, J. Pan, M. Sano, T. Takahashi, S. Hori, H. Abe, J. Hata, A. Umezawa, S. Ogawa, Cardiomyocytes can be generated from marrow stromal cells in vitro, J. Clin. Invest. 103 (1999) 697–705.
[4] J.K. Yamashita, M. Takano, M. Hiraoka-Kanie, C. Shimazu, Y. Peishi, K. Yanagi, A. Nakano, E. Inoue, F. Kita, S. Nishikawa, Prospective identification of cardiac progenitors by a novel single cell-based cardiomyocyte induction, FASEB J. 19 (2005) 1534–1536.
[5] S.J. Kattman, T.L. Huber, G.M. Keller, Multipotent flk-1+ cardiovascular progenitor cells give rise to the cardiomyocyte, endothelial, and vascular smooth muscle lineages, Dev. Cell 11 (2006) 723–732.
[6] Y.N. Tallini, K.S. Greene, M. Craven, A. Spealman, M. Breitbach, J. Smith, P.J. Fisher, M. Steffey, M. Hesse, R.M. Doran, A. Woods, B. Singh, A. Yen, B.K. Fleischmann, M.I. Kotlikoff, C-kit expression identifies cardiovascular precursors in the neonatal heart, Proc. Natl. Acad. Sci. USA 106 (2009) 1808–1813.
[7] G.L. Radice, H. Rayburn, H. Matsunami, K.A. Knudsen, M. Takeichi, R.O. Hynes, Developmental defects in mouse embryos lacking N-cadherin, Dev. Biol. 181 (1997) 64–78.
[8] T. Mori, T. Kiyono, H. Imabayashi, Y. Takeda, K. Tsuchiya, S. Miyoshi, H. Makino, K. Matsumoto, H. Saito, S. Ogawa, M. Sakamoto, J. Hata, A. Umezawa, Combination of hTERT and bmi-1, E6, or E7 induces prolongation of the life span of bone marrow stromal cells from an elderly donor without affecting their neurogenic potential, Mol. Cell. Biol. 25 (2005) 5183–5195.
[9] K. Okamoto, S. Miyoshi, M. Toyoda, N. Hida, Y. Ikegami, H. Makino, N. Nishiyama, H. Tsuji, C.H. Cui, K. Segawa, T. Uyama, D. Kami, K. Miyado, H. Asada, K. Matsumoto, H. Saito, Y. Yoshimura, S. Ogawa, R. Aeba, R. Yozu, A. Umezawa, 'Working' cardiomyocytes exhibiting plateau action potentials from human placenta-derived extraembryonic mesodermal cells, Exp. Cell Res. 313 (2007) 2550–2562.
[10] Y. Takeda, T. Mori, H. Imabayashi, T. Kiyono, S. Gojo, S. Miyoshi, N. Hida, M. Ita, K. Segawa, S. Ogawa, M. Sakamoto, S. Nakamura, A. Umezawa, Can the life span of human marrow stromal cells be prolonged by bmi-1, E6, E7, and/or telomerase without affecting cardiomyogenic differentiation?, J Gene Med. 6 (2004) 833–845.
[11] J.T. Yang, H. Rayburn, R.O. Hynes, Cell adhesion events mediated by alpha 4 integrins are essential in placental and cardiac development, Development 121 (1995) 549–560.
[12] L. Kwee, H.S. Baldwin, H.M. Shen, C.L. Stewart, C. Buck, C.A. Buck, M.A. Labow, Defective development of the embryonic and extraembryonic circulatory systems in vascular cell adhesion molecule (VCAM-1) deficient mice, Development 121 (1995) 489–503.
[13] N. Takakura, H. Yoshida, Y. Ogura, H. Kataoka, S. Nishikawa, PDGFR alpha expression during mouse embryogenesis: immunolocalization analyzed by whole-mount immunohistostaining using the monoclonal anti-mouse PDGFR alpha antibody APA5, J. Histochem. Cytochem. 45 (1997) 883–893.
[14] T.M. Liu, Y.N. Wu, X.M. Guo, J.H. Hui, E.H. Lee, B. Lim, Effects of ectopic Nanog and Oct4 overexpression on mesenchymal stem cells, Stem Cells Dev. 18 (2009) 1013–1022.
[15] C.C. Tsai, P.F. Su, Y.F. Huang, T.L. Yew, S.C. Hung, Oct4 and Nanog directly regulate Dnmt1 to maintain self-renewal and undifferentiated state in mesenchymal stem cells, Mol. Cell 47 (2012) 169–182.
[16] M.J. Go, C. Takenaka, H. Ohgushi, Forced expression of Sox2 or Nanog in human bone marrow derived mesenchymal stem cells maintains their expansion and differentiation capabilities, Exp. Cell Res. 314 (2008) 1147–1154.
[17] J. Li, V.V. Patel, I. Kostetskii, Y. Xiong, A.F. Chu, J.T. Jacobson, C. Yu, G.E. Morley, J.D. Molkentin, G.L. Radice, Cardiac-specific loss of N-cadherin leads to alteration in connexins with conduction slowing and arrhythmogenesis, Circ. Res. 97 (2005) 474–481.
[18] M. Honda, A. Kurisaki, K. Ohnuma, H. Okochi, T.S. Hamazaki, M. Asashima, N-cadherin is a useful marker for the progenitor of cardiomyocytes differentiated from mouse ES cells in serum-free condition, Biochem. Biophys. Res. Commun. 351 (2006) 877–882.
[19] J. Sterneckert, S. Hoing, H.R. Scholer, Concise review: Oct4 and more: the reprogramming expressway, Stem Cells 30 (2012) 15–21.
[20] A.P. Soler, K.A. Knudsen, N-cadherin involvement in cardiac myocyte interaction and myofibrillogenesis, Dev. Biol. 162 (1994) 9–17.
[21] K. Imanaka-Yoshida, K.A. Knudsen, K.K. Linask, N-cadherin is required for the differentiation and initial myofibrillogenesis of chick cardiomyocytes, Cell Motil. Cytoskeleton 39 (1998) 52–62.
[22] K.K. Linask, K.A. Knudsen, Y.H. Gui, N-cadherin-catenin interaction: necessary component of cardiac cell compartmentalization during early vertebrate heart development, Dev. Biol. 185 (1997) 148–164.
[23] T. Volk, B. Geiger, A-CAM: a 135-kD receptor of intercellular adherens junctions. I. Immunoelectron microscopic localization and biochemical studies, J. Cell Biol. 103 (1986) 1441–1450.
[24] S.B. Geisler, K.J. Green, L.L. Isom, S. Meshinchi, J.R. Martens, M. Delmar, M.W. Russell, Ordered assembly of the adhesive and electrochemical connections within newly formed intercalated disks in primary cultures of adult rat cardiomyocytes, J. Biomed. Biotechnol. 2010 (2010) 624719.
[25] H. Gerhardt, H. Wolburg, C. Redies, N-cadherin mediates pericytic-endothelial interaction during brain angiogenesis in the chicken, Dev. Dyn. 218 (2000) 472–479.
[26] E. Tillet, D. Vittet, O. Feraud, R. Moore, R. Kemler, P. Huber, N-cadherin deficiency impairs pericyte recruitment, and not endothelial differentiation or sprouting, in embryonic stem cell-derived angiogenesis, Exp. Cell Res. 310 (2005) 392–400.

JOURNAL OF TISSUE ENGINEERING AND REGENERATIVE MEDICINE
J Tissue Eng Regen Med 2013; 7: 51–60.
Published online 9 February 2012 in Wiley Online Library (wileyonlinelibrary.com) **DOI:** 10.1002/term.495

RESEARCH ARTICLE

Mesenchymal stromal cells improve the osteogenic capabilities of mineralized agarose gels in a rat full-thickness cranial defect model

Norihiko Mizuta[1,2], Koji Hattori[2]*, Yoshika Suzawa[1], Soichi Iwai[1], Tomohiro Matsumoto[2], Mika Tadokoro[2], Takayoshi Nakano[3], Mitsuru Akashi[4], Hajime Ohgushi[2] and Yoshiaki Yura[1]

[1]*Department of Oral and Maxillofacial Surgery, Graduate School of Dentistry, Osaka University, 1-8 Yamadaoka, Suita, Osaka, 565-0871, Japan*
[2]*Research Institute for Cell Engineering, National Institute of Advanced Industrial Science and Technology, Amagasaki Site, 3-11-46 Nakoji, Amagasaki, Hyogo, 661-0974, Japan*
[3]*Division of Materials and Manufacturing Science, Graduate School of Engineering, Osaka University, 2-1 Yamadaoka, Suita, Osaka, 565-0871, Japan*
[4]*Division of Applied Chemistry, Graduate School of Engineering, Osaka University, 2-1 Yamadaoka, Suita, Osaka, 565-0871, Japan*

Abstract

The authors previously created HAp or $CaCO_3$ formed on or in agarose gels (HAp and $CaCO_3$ gels, respectively) as biocompatible and biodegradable bone graft materials. However, these gels have limitations for bone regeneration. Mesenchymal stromal cells (MSCs) have osteogenic potential and are considered useful for bone tissue engineering. The purpose of this study was to clarify the osteogenic abilities of MSCs loaded in HAp or $CaCO_3$ gels (MSC/HAp and MSC/$CaCO_3$ gels, respectively) using a rat cranial defect model compared to HAp and $CaCO_3$ gels alone. HAp, $CaCO_3$, MSC/Hap, and MSC/$CaCO_3$ gels were prepared for *in vivo* analyses and implanted into full-thickness bone defects created in the rat cranium. All samples were assessed radiologically and histologically at 4 and 8 weeks after implantation. Using microfocus-computed tomography, an increase in bone formation was observed in the MSC-loaded gels compared to the gels alone. In addition, peripheral quantitative computed tomography revealed higher bone mineral contents in the MSC-loaded gels compared to the gels alone. After transmission X-ray diffraction analyses, the degree of apatite *c*-axis orientation as a bone quality index of newly formed bone in the MSC-loaded gels was close to that of living cranial bone. Histologically, more extensive bone formation was detected in the MSC-loaded gels compared to gels alone. Overall, MSC/HAp and MSC/$CaCO_3$ gels showed equivalent efficacy for bone regeneration. These findings demonstrate that loading of MSCs into the gels strengthened their osteogenic ability and improved the quality of the newly formed bone. As a result, MSC-loaded gels could represent viable therapeutic biomaterials for bone tissue engineering. Copyright © 2012 John Wiley & Sons, Ltd.

Received 28 October 2010; Revised 29 March 2011; Accepted 12 July 2011

Keywords hydroxyapatite; calcium carbonate; agarose gel; tissue engineering; mesenchymal stromal cell; bone regeneration; rat cranium; bone quality

1. Introduction

The various bone defects caused by tumour resection, treatment of infection, trauma, and congenital cleft jaw are challenging problems in the field s of orthopaedic, oral, and maxillofacial surgery. Bone grafting is a vital component of many surgical procedures that facilitate the repair of bony defects (Boyne *et al.*, 1980; Zhang *et al.*, 2010). Although autologous bone grafting is a popular procedure, it has many disadvantages such as limited supply of suitable bone, requirement of a second surgical site to harvest the bone, possible postoperative complications related to the harvesting procedure, and long surgical time. To overcome these difficulties, many types of biomaterials have been developed for bone regeneration.

* *Correspondence to: Koji Hattori, Research Institute for Cell Engineering, National Institute of Advanced Industrial Science and Technology, Amagasaki Site, 3-11-46 Nakoji, Amagasaki, Hyogo 661–0974, Japan. E-mail: koji-hattori@aist.go.jp*

Hydroxyapatite (HAp) is the main inorganic component of bone and teeth, and calcium carbonate ($CaCO_3$) is the main inorganic component of mollusc shells and pearls. HAp and $CaCO_3$ are well known to show good cell adhesion, proliferation, and differentiation properties (Hott *et al.*, 1997; Hanein *et al.*, 1993). Furthermore, they have shown bone-bonding properties (Okumura *et al.* 1991; Okumura *et al.*, 1997; Ohgushi *et al.*, 1992). Based on these excellent properties, sintered HAp and $CaCO_3$ ceramics have been used as bone graft substitutes. However, these ceramics are brittle and difficult to handle. To overcome their weak mechanical properties, HAp and $CaCO_3$ can be conjugated with organic polymers such as collagens and polysaccharides to obtain elastic properties. The current authors previously developed a novel alternate soaking process for preparing organic-inorganic complexes (Taguchi *et al.* 1998; Taguchi *et al.*, 1999a, 1999b). This process was based on the widely known wet process for HAp or $CaCO_3$ formation on organic polymer hydrogels by alternate soaking in solutions containing Ca^{2+} and PO_4^{3-} or CO_3^{2-} (Ogomi *et al.*, 2003). The current study selected agarose gel as an organic polymer hydrogel because it has several advantages as a substitute for biomineralization as follows (Watanabe *et al.*, 2007). 1) It is a physically crosslinked hydrogel that does not require a chemical catalyst; 2) It is a hydrolyzable compound at a low pH; 3) It is a nonimmunogenic compound unlike animal-derived substances; and 4) It is easy to prepare and handle. Based on previous experience, this study created novel biomaterials comprised of HAp or $CaCO_3$ formed on agarose gels (HAp and $CaCO_3$ gels, respectively) as biocompatible and biodegradable bone graft materials. By *in vitro* dissolution experiments, it has been reported that HAp gel is difficult to degrade at pH 7.4; however, both HAp and $CaCO_3$ gels showed rapid degradation capabilities after *in vivo* implantation (Watanabe *et al.*, 2007; Suzawa *et al.*, 2010). Concerning the mechanical properties, the current study showed that the average breaking stress and Young's modulus of HAp gel were much greater than those of $CaCO_3$ gel (Suzawa, 2010). These data demonstrate obvious differences between HAp and $CaCO_3$ gels.

The current study showed that both HAp and $CaCO_3$ gels allowed bone healing in a partial-thickness rat cranial defect model (Suzawa *et al.*, 2010). However, the gels did not show any healing potential for full-thickness cranial defects. As a result, these gels have limitations for bone regeneration. Tissue engineering approaches involving various cells, growth factors, and biocompatible scaffolds or combinations of these components have been shown to be very effective for bone regeneration (Langer *et al.*, 1993). It is widely accepted that MSCs existing in the bone marrow are multipotent cells that are capable of differentiating into osteoblasts, chondrocytes, adipocytes, and myoblasts (Owen *et al.*, 1988; Pittenger *et al.*, 1999). Since the osteogenic potential of MSCs has been confirmed by *in vitro* culture and *in vivo* implantation, MSCs are considered useful for bone tissue engineering (Ohgushi *et al.*, 1999; Ohgushi *et al.*, 2003).

The purpose of the current study was to clarify the osteogenic abilities of MSCs loaded into HAp or $CaCO_3$ gels (MSC/HAp and MSC/$CaCO_3$ gels, respectively) using a rat cranial defect model compared to those of the gels alone, and thereby to investigate their usefulness for tissue engineering approaches.

2. Materials and methods

2.1. Formation of HAp or $CaCO_3$ on or in agarose gels

The procedure for the formation of HAp or $CaCO_3$ on agarose gels has been previously described (Tabata *et al.*, 2003). Briefly, boiled aqueous solutions containing 3% (w/v) agarose (NuSieve; Cambrex Bio Science Rockland, Rockland, ME, USA) were poured into molds created at 0.5-mm intervals between two glass slides and then cooled. The resulting agarose gels of 0.5-mm thickness were punched out into discs of 4-mm diameter. The shaped gel discs were placed into the rat cranial bone defects. To prepare HAp gels, the gel discs were alternately soaked in aqueous solutions of $CaCl_2$ (pH 7.4, 200 mmol/l) and Na_2HPO_4 (120 mmol/l) at 4 °C for 2 h followed by washing in ultrapure water after each immersion. The soaking process in each ionic solution and washing was defined as one cycle and the process was repeated alternately for 12 cycles. $CaCO_3$ gels were prepared in a similar manner, except that the gel discs were soaked in Na_2CO_3 (200 mmol/l) solution instead of Na_2HPO_4 solution. The resulting HAp and $CaCO_3$ gels were finally immersed in ultrapure water and sterilized by 25 kGy gamma-ray irradiation (Koga Isotope, Shiga, Japan) for about 2 h before cell seeding. The agarose, Hap, and $CaCO_3$ gels were analyzed using a JSM-6700FE scanning electron microscopy (SEM) (JEOL, Tokyo, Japan) (Figure 1).

2.2. MSC preparation and loading in HAp/$CaCO_3$ gels

Rat MSCs were prepared according to previously reported methods (Ohgushi *et al.*, 1996a 1996a, 1996b). Briefly, bone marrow cells were obtained from the femoral bone shafts of 7-week-old Fischer 344 male rats purchased from Japan SLC (Shizuoka, Japan). Both ends of the femoral epiphyses were cut off and the bone marrow was flushed out using 10 ml of standard medium through a 21-gauge needle. The released bone marrow cells were seeded into T-75 flasks (BD Biosciences, Bedford, MA, USA) containing 15 ml of standard medium and cultured in a humidified atmosphere of 95% air and 5% CO_2 at 37 °C. One flask was used for the cells from each femoral shaft. The standard medium consisted of minimum essential medium (MEM) (Nacalai Tesque Inc., Kyoto, Japan) supplemented with 15% foetal bovine serum (JRH Bioscience, Lenexa, KS, USA) and 1% antibiotics (100 U/ml penicillin, 100 μg/ml streptomycin, 0.25 μg/ml

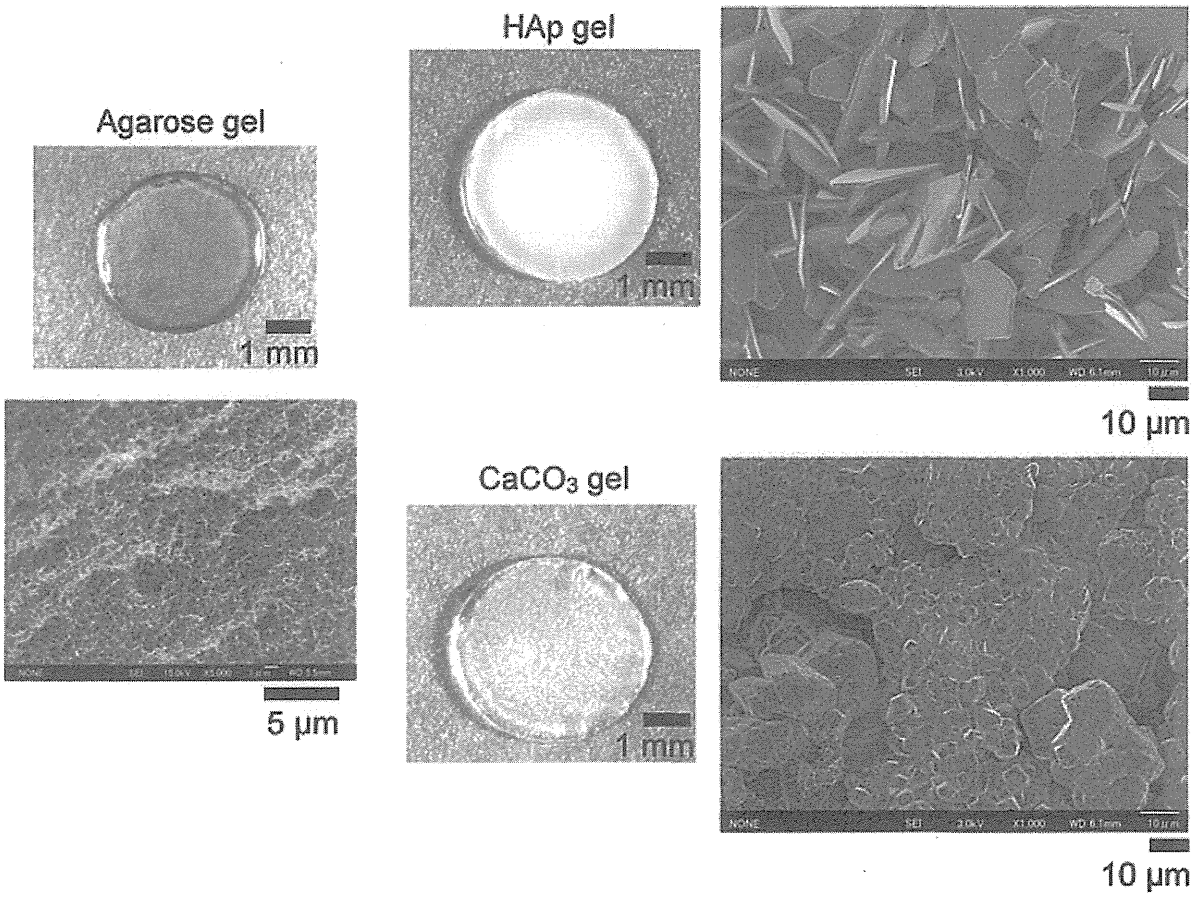

Figure 1. Macroscopic and SEM images of agarose, Hap, and $CaCO_3$ gels. The gel disks were implanted in rat full-thickness cranial defects. Crystals of HAp and $CaCO_3$ particles were observed with various sizes of diameter from about several nm to a few μM by SEM analyses

amphotericin B) (Sigma-Aldrich, St. Louis, MO, USA). To remove non-adherent cells, the medium was renewed three times per week. The cell culture was maintained for about 7 days until the cells reached confluence. It was reported that the prepared adherent cells were mesenchymal type cells with differentiation capabilities towards osteoblasts (Ohgushi *et al.*, 1996a, 1996b; Tanaka *et al.*, 2009; Kato *et al.*, 2011), vascular endothelial cells (Nagaya *et al.*, 2005), and hepatocytes (Oyagi *et al.*, 2006). The adherent cells were therefore considered as MSCs and thereby detached from the flasks using 0.05% trypsin, harvested, and resuspended in culture medium at a density of 1 x 10^7 cells/ml. Next, 1-ml aliquots of the cell suspension were applied to the disk-shaped HAp and $CaCO_3$ gels in 15-mm tissue culture plates and the mixtures were left to stand overnight in a humidified atmosphere of 95% air and 5% CO_2 at 37 °C. For preparation of the 1 x 10^7 cells, the cells were harvested from three T-75 flasks. The resulting MSC-loaded HAp and $CaCO_3$ gels (MSC/HAp and MSC/$CaCO_3$ gels, respectively) were implanted into the rat cranial defects.

2.3. Implantation

Fischer 344 male rats (8-weeks-old) were anesthetized by an intraperitoneal injection of sodium pentobarbital (Nembutal; Dainippon Pharmaceutical, Tokyo, Japan) at a final concentration of 40 mg/kg body weight. After shaving the skin, a midline incision was made in the skull and the periosteum was opened to expose the surface of the parietal bones. A 4-mm diameter full-thickness round cranial defect was created bilaterally in the parietal bone using a trephine bur (Trephine Drill; Storz am Mark Gmbh, Emmingen-Liptingen, Germany) with minimum saline irrigation. Each defect was rinsed with saline to remove any remaining debris and then implanted with the experimental gels (Figure. 2). The defects on the right side were implanted with MSC/HAp or MSC/$CaCO_3$ gels ($n = 6$). The defects on the left side were implanted with HAp or $CaCO_3$ gels without MSCs ($n = 6$ h). As controls, other cranial defects were washed with saline and left without any implants ($n = 6$). After implantation, the periosteum and skin were closed in layers with thread sutures.

The rats were returned to their cages and allowed to move freely. At 4 and 8 weeks after implantation, the rats were humanely terminated with an overdose of sodium pentobarbital and cranial bone samples were taken for the following analyses.

2.4. Microfocus-computed tomography (μ-CT)

A μ-CT imaging system for the analysis of small animals (SMX-100CT; Shimadzu, Kyoto, Japan) was used for the detection of newly formed bone in the cranial defects. The

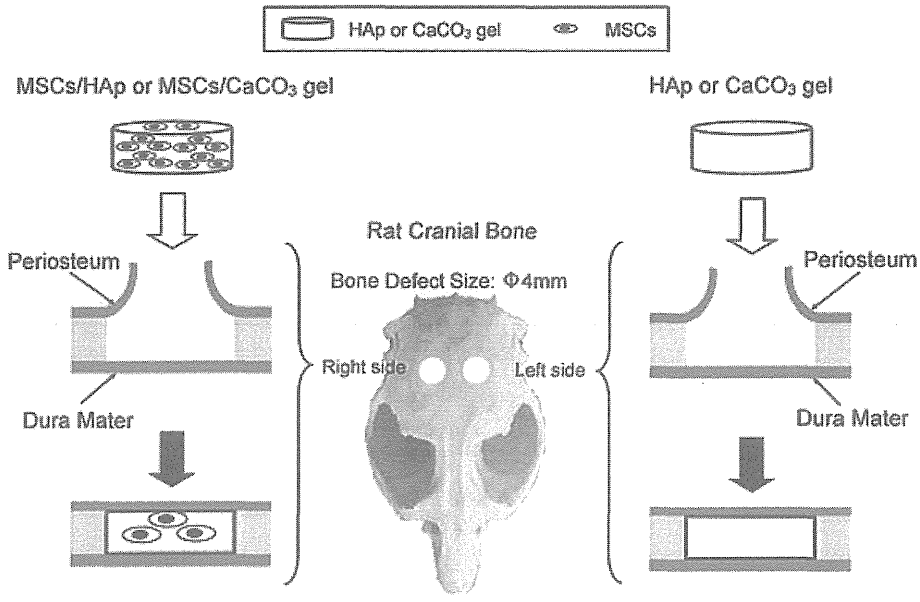

Figure 2. Schematic illustration of the rat cranial bone defect model. Full-thickness circular bone defects were produced in the rat cranial bone. The defects on the right side were implanted with MSC/HAp or MSC/$CaCO_3$ gels ($n = 6$). The defects on the left side were implanted with HAp or $CaCO_3$ gels without MSCs ($n = 6$). (MSCs, mesenchymal stromal cells; HAp gel, hydroxyapatite formed on agarose gel; $CaCO_3$ gel, calcium carbonate formed on/in agarose gel; MSC/HAp gel, MSC-loaded HAp gel; MSC/$CaCO_3$ gel, MSC-loaded $CaCO_3$ gel)

samples were scanned using a resolution of 42 μM and the isotropic voxel size was 600 views/180 degrees. The scanner was set at a voltage of 40 kV and a current of 33 μA. The sliced images were compiled and analyzed to render 3D images. Visual analyses of the μ-CT data were performed using the provided VGStudio software (Shimadzu).

2.5. Peripheral quantitative computed tomography (pQCT)

A pQCT system (XCT Research SA+, MDL922011; Stratec Medizintechnik, Pforzheim, Germany) was used to measure the volumetric bone mineral density (mg/cm^3) at arbitrary sites. Each sample was set in the gantry of the pQCT system and scanned with a 70-μM voxel size. Five serial cross-sectional slices (0.46-mm thickness) were scanned, of which the middle cross-section surface passed through the centre of the bone defect in the CT image. The scanning volume was a solid rectangle with a base of 3.96 x 1.15 mm and a height of 0.46 mm. A threshold of 267 mg/cm^3 was used to separate the newly formed bone from the surrounding tissues. The newly formed bone volume in the solid rectangle was set as the region of interest (ROI) using the ROI tool function, and the bone mineral density of the newly formed bone was determined. The bone mineral content (newly formed bone volume cm^3 x bone mineral density mg/cm^3) was used as a quantitative index in the pQCT assessment.

2.6. Microbeam X-ray diffraction (μ-XRD)

A μ-XRD system (R-AXIS BQ; Rigaku, Osaka, Japan) was used to analyze the preferential alignment of the *c*-axis of the biological apatite crystallites in the samples (Sasaki *et al.*, 2008). Molybdenum (Mo)-Kα radiation was generated at a tube voltage of 50 kV and a tube current of 90 mA, and the incident beam was focused onto a beam spot of 800 μM in diameter by a collimator. The beam was vertically directed against the surface of the newly formed bone that existed in each defect. Using the diffraction profile measured in an anteroposterior direction of the skull, the intensities of the (002) and (310) peaks were detected, and the integral intensity ratio (002/310) was calculated. Nakano *et al.* (2002) reported that the preferential alignment of the *c*-axis of biological apatite crystallites is strongly dependent on bone sections such as long bone, flat bone, or dentulous mandible, and can be assessed by the relative intensities between the (002) and (310) diffraction peaks. An increase in the relative intensity ratio indicated more frequent alignment of the *c*-axis of the biological crystallites.

2.7. Histological and histomorphometric analyses

The samples were fixed in 10% neutral-buffered formalin, decalcified with K-CX solution (Falma, Tokyo, Japan), and embedded in paraffin. Sagittal sections (4-μm thick) were prepared from the centre of the defects and stained with hematoxylin and eosin. For histomorphometric analysis, the newly formed bone areas in the defects were measured using Image-Pro® Plus J image software (Media Cybernetics, Bethesda, MD, USA). The bone area ratio (area of newly formed bone/area of cranial defect in the histological section) was used as a quantitative index in the histomorphometric assessment.

2.8. Statistical analysis

For comparisons between HAp or $CaCO_3$ gels alone and MSC/HAp or MSC/$CaCO_3$ gels, the differences were analyzed by the nonparametric Mann-Whitney U test. The significance level was set at $P < 0.05$.

3. Results

3.1. μ-CT findings

At 4 weeks after implantation, the radioopaque areas were larger in the MSC/HAp gels than in the HAp gels alone. Similarly, the radioopaque areas were larger in the MSC/$CaCO_3$ gels than in the $CaCO_3$ gels alone. At 8 weeks after implantation, the same tendencies were observed and the MSC-loaded gels contained larger radioopaque areas than the gels without MSCs. The radio-opacities of the MSC/HAp and MSC/$CaCO_3$ gels at 8 weeks after implantation were higher than those at 4 weeks after implantation. In defects without any implants, almost all areas were radiolucent at both 4 and 8 weeks after implantation (Figure 3, Defect).

3.2. pQCT findings

Figure 4 shows the data obtained in the pQCT analyses. At 4 weeks after implantation, the mean bone mineral contents were 824 mg in MSC/HAp gels, 284 mg in HAp gels, 918 mg in MSC/$CaCO_3$ gels, 411 mg in $CaCO_3$ gels, and 119 mg in defects without gels (Defect). Significant differences were found between MSC/HAp and HAp gels and between MSC/$CaCO_3$ and $CaCO_3$ gels. At 8 weeks after implantation, the mean bone mineral contents were 1019 mg in MSC/HAp gels, 464 mg in HAp gels, 1150 mg in MSC/$CaCO_3$ gels, 500 mg in $CaCO_3$ gels, and 192 mg in defects without gels (Defect). Significant differences were observed between MSC/HAp and HAp gels and between MSC/$CaCO_3$ and $CaCO_3$ gels.

3.3. μ- XRD findings

Figure 5 shows the integral intensity ratios of (002/310) corresponding to the degrees of preferential *c*-axis alignment in the newly formed bone. At 4 weeks after implantation, the mean integral intensity ratios of (002/310) were 1.5 in MSC/HAp gels, 0.35 in HAp gels, 1.45 in MSC/$CaCO_3$ gels, and 0.39 in $CaCO_3$ gels. Significant differences were found between MSC/HAp and HAp gels and between MSC/$CaCO_3$ and $CaCO_3$ gels. At 8 weeks after implantation, the mean integral intensity ratios of (002/310) were 1.9 in MSC/HAp gels, 0.52 in HAp gels, 1.7 in MSC/$CaCO_3$ gels, and 0.55 in $CaCO_3$ gels. Significant differences were found between MSC/HAp and HAp gels and between MSC/$CaCO_3$ and $CaCO_3$ gels.

3.4. Histological and histomorphometric findings

Histological and histomorphometric findings are shown in Figures 6 and 7, respectively. At 4 weeks after

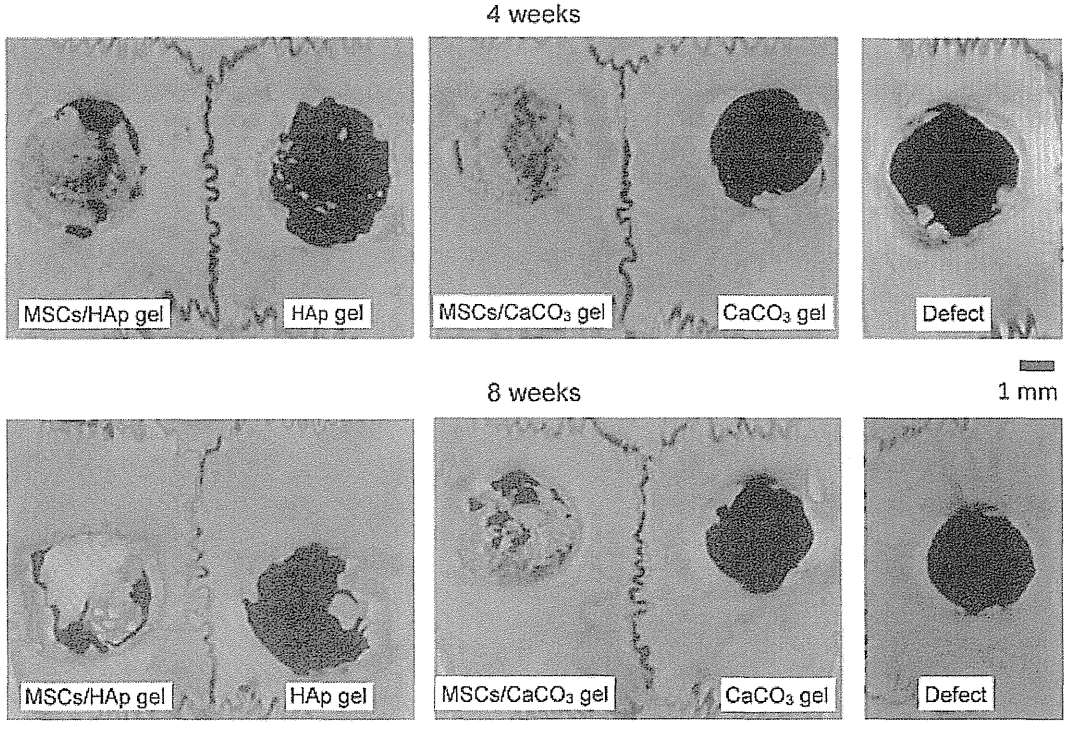

Figure 3. μ-CT images of rat calvariae. Upper panels: images at 4 weeks after implantation; lower panels: images at 8 weeks after implantation. Defect: cranial defects without any implants